Dye-Sensitized Solar Cells Based on a Single-Crystalline TiO_2 Nanorod Film

Jinting Jiu,*,† Seiji Isoda,† Fumin Wang,‡ and Motonari Adachi*,§

Institute for Chemical Research, Kyoto University, Uji, Kyoto 611-0011, Japan, School of Chemical Engineering and Technology, Tianjin University, Tianjin 300072, People's Republic of China, and International Innovation Center, Kyoto University, Yoshida-Honmachi, Sakyo, Kyoto 606-8501, Japan

Received: October 12, 2005; In Final Form: November 15, 2005

Highly crystalline TiO_2 nanorods with lengths of 100−300 nm and diameters of 20−30 nm have been synthesized by a hydrothermal process in a cetyltrimethylammonium bromide surfactant solution. The microstructure measured by X-ray diffraction and high-resolution transmission electron microscopy was a pure highly crystalline anatase phase with a long nanorod shape. The addition of a triblock copolymer poly(ethylene oxide)$_{100}$−poly(propylene oxide)$_{65}$−poly(ethylene oxide)$_{100}$ (F127) decreased the length of the nanorods and kept the rod shape of the particles even after sintering at high temperatures. The rod shape kept under high calcination temperatures contributed to the achievement of the high conversion efficiency of light-to-electricity as discussed in the paper. A high conversion efficiency of light-to-electricity of 7.29% was obtained with the TiO_2 single-crystalline anatase nanorod cell.

Introduction

Dye-sensitized solar cells (DSSC) based on mesoporous TiO_2 electrodes are currently attracting widespread and intense academic and industrial interest for the conversion of sunlight into electricity because of their low cost and environmentally friendly photovoltaics with good efficicencies comparable to those of silicon cells.[1] These DSSCs usually consist of a mesoporous anode formed by a sintered film of anatase TiO_2 that serves as the electron acceptor and a transport layer coated with a thin layer of sensitizer-dye molecules for light absorption and electron injection into the TiO_2 conduction band. A liquid electrolyte generally consists of an organic solvent such as acetonitrile and a redox couple I^-/I_3^- that serves as a redox agent to reduce the photoexcited dye molecules. In the cells, undoubtedly, mesoporous titania films and dyes are two of the key components for high-power-conversion efficiencies. The amount of dye covered on the surface of TiO_2 will determine the adsorption efficiency of sunlight, which is related to the number of electrons excited in cells. However, preparation methods of TiO_2 film affect the pore size distribution, porosity, and crystallinity, and then all of these will correlate with the transport of electrons and diffusion of electrolyte in the cells. Recently, research efforts have focused on improving this system by altering the particle size and morphology of TiO_2,[2−3] optimizing the fabrication and structure of the TiO_2 film,[4] developing new sensitizers,[5] suppressing charge recombination,[6] and improving interfacial energetics.[7] A high-performance DSSC requires nanoscale and highly crystalline TiO_2 electrodes with large surface areas and favorable electrical contiguity with conducting glass substrates so that dyes can be sufficiently adsorbed and electrons can be quickly transferred. So far, according to the above concept, TiO_2 film electrodes with spherical nanoparticles have been prepared commonly from colloids with the doctor-blade technique, which makes it possible to fabricate porous electrodes with high surface areas. However, TiO_2 nanocrystals with other morphologies have been scarcely reported in dye-sensitized solar cells. It is known in the realm of nanoscience and nanotechnology that nanorods, nanowires, and nanotubes play special roles because of their one-dimensionality. When the diameter of the nanorod, nanowire, or nanotube becomes small, the physico-chemical properties of the one-dimensional nanostructure are clearly different from those of crystalline solids or even two-dimensional systems, resulting in novel quantum phenomena and inconceivable properties. A bismuth nanowire is an excellent example, which transforms into a semiconductor as the wire diameter becomes smaller.[8] Meanwhile, it was pointed out that such a nanowire might be constructed of isoelectronic materials that permit easy electron transport along the nanowire.[8] However, we know that DSSCs are a rather complicated system including such processes in a series as light adsorption, charge injection, charge transport, charge collection, and electrolyte diffusion. Accordingly, there are many factors that influence the resultant light-to-electricity conversion efficiency of DSSCs. Furthermore, when considering only the electron transport in the mesoporous TiO_2 film, we need to consider many factors such as the surface state of the particles, the channel and connection between particles, and the morphology of the particles, because they change many electrical and physical properties of the system. Aside from the inconceivable properties of one-dimensional materials, we believe that the use of highly crystalline anatase nanorods is one of the most promising routes to higher efficiency, because the barrier effect of intercrystalline titania is greatly decreased by using a long single-crystalline nanorods instead of a porous titania thin film composed of accumulated nanosized particles. This might contribute to easier electron transfer and decrease the ohmic loss through the titania layer. Recently, we have reported that high efficiency had been achieved with TiO_2 nanowires composed of many nanoparticles aligned with each other due to "oriented attachment" growth, which implied the electron

* Authors to whom correspondence should be addressed. Phone: +81 774 383052 (J.J.); +81 774 384358 (A.M.). Fax: +81 774 383055 (J.J.); +81 774 383055 (A.M.). E-mail: jiu@eels.kuicr.kyoto-u.ac.jp; adachi@iae.kyoto-u.ac.jp.

† Institute for Chemical Research, Kyoto University.

‡ Tianjin University.

§ International Innovation Center, Kyoto University.

10.1021/jp055824n CCC: $33.50
Published on Web 01/13/2006

transfer in TiO_2 film is an important parameter for DSSCs.[2] Hence, we attempted to prepare nanorods, as a substitute for oriented attachment nanoparticles, and evaluate the performance of nanorod DSSCs.

Experimental Section

First cetyltrimethylammonium bromide (CTAB) was dissolved in distilled water at 308 K, and the concentration was fixed at 0.005−0.1 M. After a transparent solution was obtained, titanium isopropoxide (TIPT, 0.22 M) was added immediately into the above CTAB solution with stirring under ethylenediamine (EDA) basic catalyst. White precipitation obtained by hydrolyzation of TIPT was then transferred into a Teflon autoclave, sealed with a crust made of stainless steel, and reacted at 433 K for 6−12 h to nucleate and grow titania particles. The resulting white solid product was used for the formation of film electrodes as reported[9] by adjusting the concentration of TiO_2 in the last suspension. In the experiment, we found that the diameter and length of nanorod can be controlled by mixing a triblock copolymer of poly(ethylene oxide)$_{100}$−poly(propylene oxide)$_{65}$−poly(ethylene oxide)$_{100}$ (F127) with CTAB in the beginning, and these results will be discussed mainly in the present paper.

Characterization. The obtained samples were characterized by X-ray powder diffraction (XRD) using a Rigaku goniometer (PMG-A2, CN2155D2) X-ray diffractometer with Cu Kα radiation ($\lambda = 0.154$ nm) at a scan rate of 2° min^{-1}. The morphology and features of the product peeled from the cells were examined using transmission electron microscopy (TEM; JEOL 200CX) with an acceleration voltage of 200 kV and scanning electron microscopy (SEM; JEOL JSM-6500FE). The photocurrent−voltage characteristics were measured using an AM 1.5 solar simulator (Bunkoh-Keiki Co. Ltd., CEP-2000) in which the light intensity is 100 mW/cm^2, calibrated with a standard silicon solar photodiode (BS520, Bunkoh-Keiki Co. Ltd.). The cell size was 0.25 cm^2. The composition of the electrolyte was 0.1 M LiI, 0.6 M 1,2-dimethyl-3-*n*-propylimidazolium iodide (DMPII), 0.05 M I_2, and 0.5 M 4-*tert*-butylpyridine (TBP) in methoxyacetonitrile.

Results and Discussion

Formation of Nanocrystalline TiO_2 Nanorods. It is known that the wet-chemical technique is favored as an appropriate process for preparing nanostructured materials because particle size, morphology, and structures can be controlled by adjusting preparation parameters, although TiO_2 with different shapes such as nanorods,[10] nanowires,[11] and nanotubes[12] have been synthesized by different physical or hard-template methods. Alternatively, nanocrystal shape evolution in a controllable manner using the wet-chemical technique with a soft template is also an interesting and attracting research subject. Low-dimensional shape formation, such as a rod, requires anisotropic crystal growth, which is realized usually when the surface free energies of the various crystallographic planes differ significantly. Recently, Puntes et al.[13] showed that the formation of a tetrapod structure could be realized in the case of CdSe by using two different surface ligands that probably bind selectively to the respective surface planes. Also Jun et al.[14] showed that the shape evolution of titanium dioxide anatase nanocrystals from bullet and diamond structures to rods and branched rods could be achieved by modulating the surface energies of the different crystallographic faces with a surface selective surfactant, which is the key parameter for shape control. In such a way, development of shape evolution with selective surfactants in wet-chemical methods is an attractive topic in the preparation process of nanoscale materials. In general, the highest-energy facets are eliminated during crystal growth so that progressive addition of a selective surfactant should yield a sequence of shapes. It is known that TiO_2 anatase has a tetragonal structure (the *c*-axis being 2.7 times the *a*-axis) and has been shown to nucleate as truncated octagonal bipyramidal seeds, exposing eight equivalent {101} faces and two equivalent {001} faces.[15] According to Donnay−Harker rules,[16] the surface free energy of the {001} faces is nearly 1.4 times larger than that of the {101} faces. Therefore, these features determine the intrinsic instability of the nucleus; the shape evolution in TiO_2 anatase can be realized by modifying the surface free energy and growth rate of the nucleus with the surface adhesion of ligands.

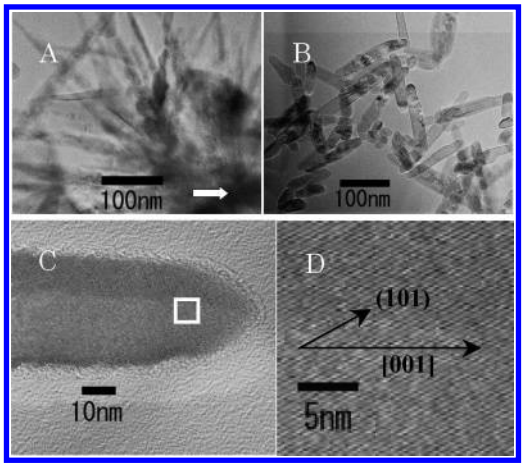

Figure 1. TEM images of nanorods prepared in CTAB (A) without and (B) with F127 and (C and D) HRTEM image of nanorod formed with F127.

Our proposed process is based on the interaction between a titania precursor nucleus, surfactant CTAB, and copolymer F127 under basic conditions in a hydrothermal environment. At low concentrations of CTAB, irregular spherical (0.005 M) and short rod (0.03 M) nanocrystals are obtained. When the amount of CTAB is increased up to 0.05 M, the formation of long branched rods is observed with diameters of 20−30 nm and lengths of over 500 nm (Figure 1A). When a large excess of CTAB is used (over 0.1 M), only sphere-shaped nanocrystals can be obtained. When the copolymer F127, which exhibits a strong adhesion on the surface of the oxide, is added into the system of 0.05 M CTAB, the branched rods in Figure 1A are completely dispersed into single rods with the same diameter and slightly shorter lengths (Figure 1B). These nanorods are expected to be beneficial for the transfer of electrons in the rods. Figure 1C shows a high-resolution TEM (HRTEM) image of a single TiO_2 nanorod obtained with F127, and the end of the nanorod is not clearly truncated but a tip shape. The observed clear lattice fringes (Figure 1D, a magnified image of the selected square area indicated in Figure 1C) indicate that the nanorods exhibit high crystallinity with a few defects such as microtwins. The fringes are (101) planes with a lattice spacing of about 0.354 nm. The long direction of the nanorod is along the [001] direction. Hence, the end of the nanorod in Figure 1C is along the (100) plane, which agrees with repeating octahedral bipyramidal units in anatase phase TiO_2.[17]

X-ray diffraction patterns of the samples indicate also the presence of nanocrystalline anatase with a typical anisotropic growth pattern along the [001] direction. A gradual increase in the relative (004)/(200) intensities was observed as the nanocrystal shape evolves from irregular spheres to short rods to long rods, as a consequence of the extended crystalline domain

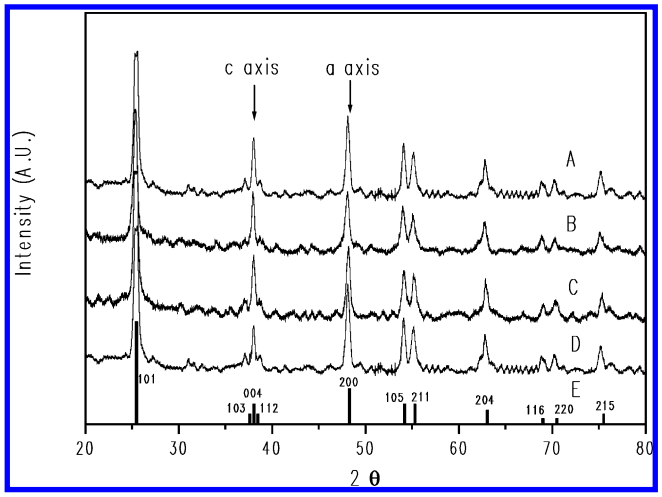

Figure 2. XRD patterns of nanorods (A) without and (B) with F127 before calcination, (C) with and (D) without F127 after calcination at 450 °C, and (E) spherical particles of antase TiO_2.

along the *c*-axis. Figure 2 shows the XRD pattern (Figure 2A) without and (Figure 2B) with F127 in 0.05 M CTAB. From Figure 1A, it can be seen that the long rod is over 500 nm in length, in comparison to 100−150 nm in Figure 1B. However, the former gives an intensity ratio of (004)/(200) of only 0.84, which is smaller than that with the shorter rods in Figure 1B. It hints that the branched rods include a part of bulk titania as observed in Figure 1A (white arrow). After the addition of F127, the rods can be completely dispersed into single rods with a high intensity ratio of (004)/(200) reflections. And these single nanorods are limited in a range of short length with the same diameter, which also indicates a reason for shape control in nanocrystal formation with two or more ligands in the wet-chemical method.[13,14] In our case, it can be expected also that the direction of crystal growth of nanorods is improved by the adsorption of the surfactant CTAB and F127 on the surfaces of TiO_2.

Application of Nanorods to DSSCs. Since a DSSC is a rather complicated system, there are many factors that influence the resultant light-to-electricity conversion efficiency. Among them, the TiO_2 electrode is a key parameter in a DSSC. Since the morphology, diameter, surface state, and porosity of the TiO_2 film will affect the electron transport and electrolyte diffusion in the cell, further development of preparation techniques for the nanocrystalline TiO_2 films is desired. Among many possible approaches, the use of a highly crystalline anatase nanorods, nanowires, or nanotubes is anticipated to be one of the most promising ways, because the interconnections between crystalline titania particles are greatly decreased by using a single-crystalline and one-dimensional nanorod, nanotube, or nanowire in comparison with a porous titania thin film composed of accumulated nanosized particles. This might be useful for easier electron transfer through the one-dimensional and optimized structure titania film.[2] Furthermore, the titania film with random packing of one-dimensional rods is also expected to enhance the diffusibility of electrolyte in the cell because the porosity and structures of pores are improved from that composed of many very small particles. On the basis of the above consideration, we have attempted to fabricate a cell based on the highly crystalline TiO_2 nanorods prepared with the above hydrothermal method. To estimate the performance of the cell composed of the titania nanorods, a cell composed of standard P-25 titania particles was fabricated as a reference. The photocurrent−voltage characteristics of both cells were measured under the same experimental conditions.

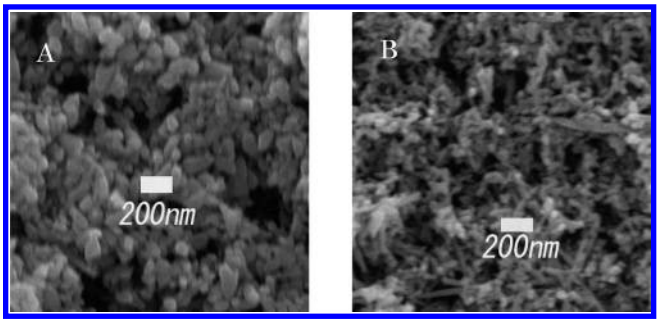

Figure 3. SEM images of nanorod films formed (A) without and (B) with F127 after calcination at 450 °C.

Figure 3 shows the SEM images of the surface morphology of TiO_2 nanorod film (Figure 3A) without and (Figure 3B) with F127 after calcination at 450 °C for 1 h. It is clear that the system with F127 kept the rod shape well even at a high calcination temperature (Figure 3B), and surprisingly we found that the rod shape is not destroyed even with 550 °C sintering process. The XRD pattern of nanorods after calcination supports the result (Figure 2C). For the sample with F127, the intensity ratio of (004)/(200) is 0.965, which is also as high as that of nanorods before the calcination and much higher than that (0.57) of spherical particles (Figure 2E). Contrarily, the rod shape is completely destroyed for the system without F127. Only irregular and large spherical particles are produced, so that the XRD pattern indicates that the ratio of (004)/(200) is drastically decreased and is very low at 0.68 (Figure 2D). When the intensity ratio in spherical particles of 0.57 is compared, it is still high, suggesting that the irregular and large spherical particles still grow along the *c*-axis direction. Although it is not clear why the rod shape is kept for the sample prepared with F127, there could be two reasons. One is the strain probably distributed around these trunk rods, which leads to crushing of the rod-shaped particles by applying heat. Another is the adsorption of surfactants on the surfaces of the rod particles. In the CTAB and F127 system, the surfaces of the rod particles are tightly and wholly covered with the two surfactants, resulting in excellent single-crystalline nanorods free from defects and strain, even during calcination as observed by HRTEM (Figures 1C and 1D). However, the mechanism should be studied in the future. In any case, considering the rod shape in our case, the nanorods prepared with F127 will be advantageous to fabricate the electrode film.

Figure 4 shows the short-circuit current density and efficiency obtained from the cells made of the titania nanorods with N719 dye, together with those of P-25, against the film thickness. In the thin film region, the current densities of the two cells are nearly the same, and the P-25 cell has an even slightly higher current density. However, the current density gradually increases in nanorod DSSCs when the film thickness is over 8 μm (Figure 4). Similarly, the efficiency of the nanorods is largely increased with thick film when comparing the case of P-25 cells.

Figure 5 shows the short-circuit current density obtained for both cells as a function of the amount of dye adsorbed on the titania thin film per unit area of the conducting glass. In the adsorption range from 0 to 6×10^{-8} mol/cm^2, both cells exhibit almost the same photocurrent density. Contrary to this, in the higher dye amount range, the photocurrent density of the P-25 cell stops increasing and becomes flat, while the photocurrent density of the nanorod DSSC gives a linear increase. The saturation in the P-25 cell indicates that the recombination of electrons is drastically increased due to the thicker film including many more connection barriers between titania particles, which

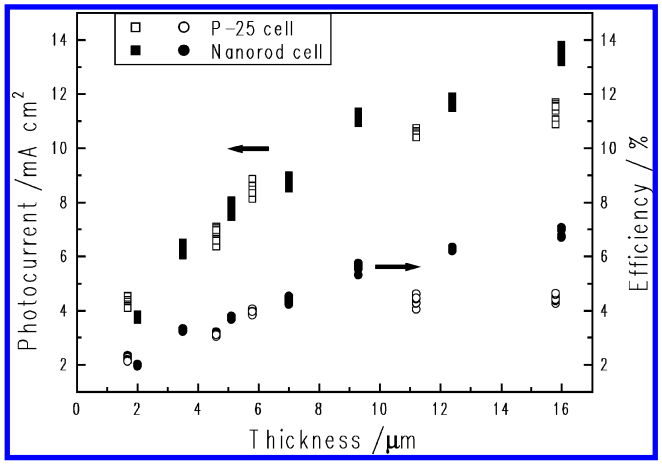

Figure 4. Dependences of the photocurrent density (■ nanorod, □ P-25) and efficiency (● nanorod, ○ P-25) on the thickness of film in nanorod and P-25 cells.

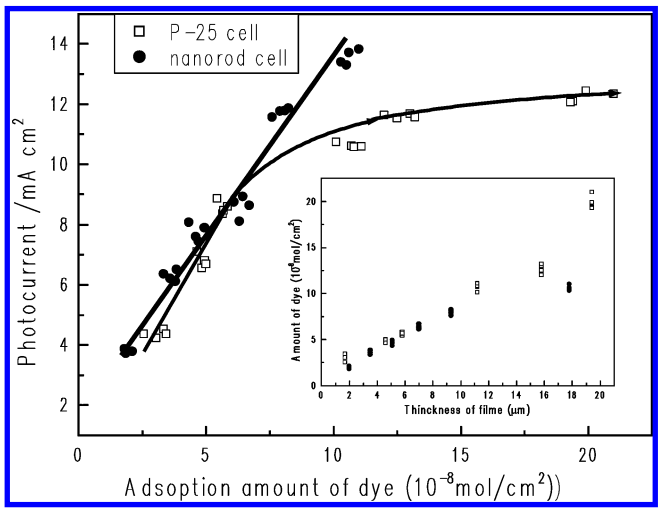

Figure 5. Relationship between the photocurrent density and the dye amount adsorbed. The inset shows the dependence of dye amount on the thickness of the film.

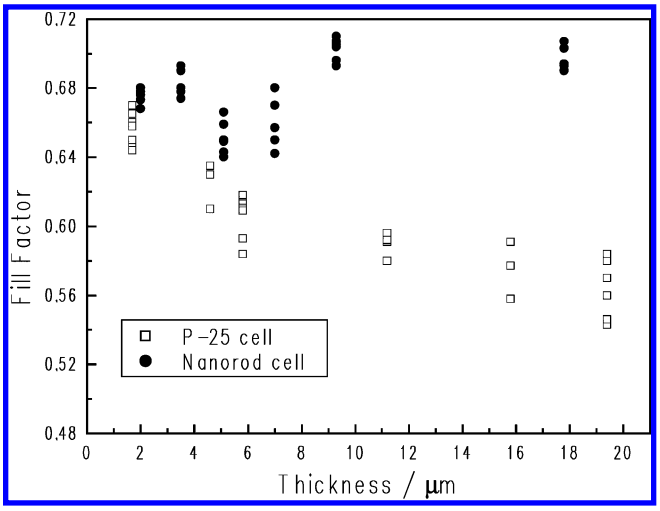

Figure 6. Fill factors of nanorod and P-25 cells.

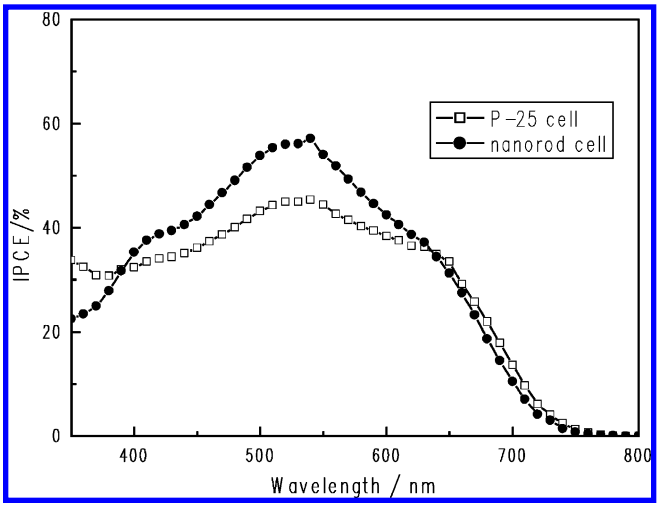

Figure 7. IPCE of nanorod and P-25 cells.

usually formed grain boundaries acting as electron traps. The linear increase in the high dye concentration region of this cell with TiO_2 nanorods means potentially higher efficiency. However, the adsorbed amount of dye in nanorods is the same or somewhat smaller in comparison to that of the P-25 cell with the same film thickness. The relationship between the film thickness and the adsorbed N719 dye amount is shown in the inset in Figure 5. The adsorbed N719 dye was measured by dissolving completely from the TiO_2 film to a 0.1 M sodium hydroxide aqueous solution, and the concentration of N719 was determined by a spectroscopic method. In the thin range from 0 to 10 μm, the amount of dye adsorbed to the titania nanorod film is almost same as that of the P-25 film. The Brunauer−Emmett−Teller (BET) specific surface areas of the calcined titania nanorods and P-25 are 40 and 55 m^2/g, respectively. Thus, the titania nanorods do not adsorb much higher amount of dyes than the P-25 film although one needs to remember that the nanorods have higher crystallinity.[18−19] However, the amount of adsorbed dye per unit area in nanorod film is more than that in the P-25 film from the consideration of the porosity and the surface areas of the two materials. And the nitrogen adsorption/desorption measurement shows the larger pore volume of 638.7 mm^3/g in nanorod film than that of 187.9 mm^3/g in the P-25 film, which suggests that the former has much less surface area with same film thickness. But the film adsorbed almost same amount of dye like the P-25 film with the larger surface areas showed the inset of Figure 5. We believe here that the high crystallinity of the nanorod film is the most essential reason. And the pore structure of the nanorod film composed of the randomly packing nanorods also is a factor for more adsorption of the dye as mentioned previoudly.[20] Meanwhile, the rutile phase included in the P-25 film is another reason affecting the adsorption of the dye in the P-25 film as compared to the pure anatase phase in the nanorod film. Hence, the surface area, phase, as well as morphology in the nanorod film determine the adsorbed amount of dye in the films, which achieves more electrons injecting in the cell. Except the effect of the adsorbed dye amount, the high current density in nanorod cells is also related to the light scattering effect in the rod-packed structure due to the large size of the nanorod particles. However, we could not obtain the evidence from the incident photon to current conversion efficiency (IPCE) spectra showed in Figure 7. The IPCE spectra indicated that the value is 2−4% lower in the nanorod cell than that in the P-25 cell in the long wavelength region (650−750 nm). Generally, the enhanced IPCE was attributed to the light scattering effect in the region. Contrarily, in the short wavelength region (400−600 nm), a high IPCE value has been achieved in the nanorod cell. It hinted that the high current density might be attributed to the very high rate of electron transfer through the single-crystalline TiO_2 nanorods. When the nanoparticles are compared, the long-shaped particles such as the nanorod, nanowire, or nanotube are constructed of

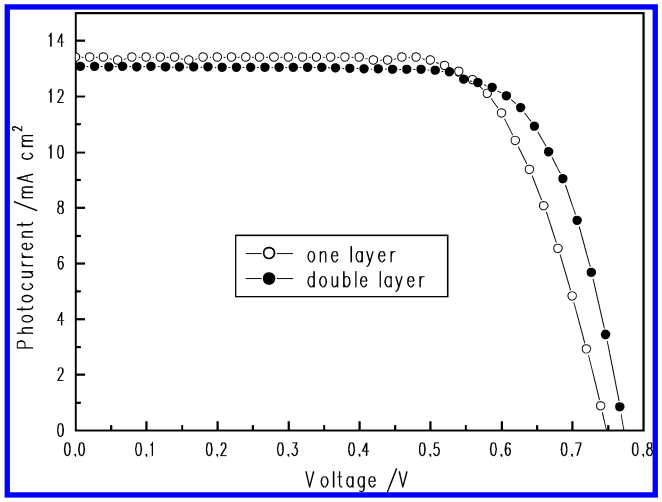

Figure 8. *I*−*V* curves of nanorod cells.

isoelectronic materials that permit easy electron transport along the long direction.[8] So far, the use of TiO_2 nanorods with high crystallinity instead of TiO_2 nanoparticles results in the decreased number of contact barriers between titania material, which usually forms grain boundaries acting as electron traps. This point is confirmed by measuring the fill factor for the nanorod and P-25 cells. The result is shown in Figure 6. The fill factor relates closely with the total series resistance of cell. When the electrons can be quickly transported without large resistance, the value of the fill factor is increased, otherwise the value will be decreased. When the results for the P-25 and nanorod DSSC are compared, the fill factor is lower in the former with increasing thickness of the film, which indicates that the resistance generally increased with the semiconductive TiO_2 nanoparticle layer by including many more contacting points between particles. Not only for thick film, the fill factor is always larger in the nanorod DSSC, suggesting that the nanorods are an excellent candidate for the rapid transportation of electrons. Meanwhile, it should be considered that the fill factor is determined by a large variety of factors, for example, the resistance of the substrate and the quality of the counter electrode. Hence, the high fill factor is considered also to contribute to the creation of an ample ion path for the redox agent I^-/I_3^- in the nanorod layer because it can make a rod-shaped long path for ion penetration particularly when thicker films are examined. Figure 8 shows the current−voltage characteristics obtained for the cell with a TiO_2 thin film composed of single-crystalline anatase nanorods. The titania thin film was prepared by directly coating the rod gel several times on indium tin oxide (ITO) conductive glass with a suitable thickness. The sample was calcined after every coating at 450 °C for 10−15 min, and at last the film was calcined for 60 min. And then the film was immersed into N719 dye solution over 20 h. A high light-to-electricity conversion rate of 7.06% is obtained for the cell with TiO_2 single-crystalline anatase nanorods of 16 μm in thickness. Short-circuit photocurrent density, open-circuit voltage, and fill factor are obtained as 13.4 mA/cm^2, 0.748 V, and 0.703, respectively. This high light-to-electricity conversion is attributed to the single-crystalline anatase nanorods shown in Figure 1. To obtain better performance from a DSSC, a compact TiO_2 layer prepared by the sol−gel method was reported to be effective, and a dense TiO_2 layer based on the reactive direct current magnetron sputter deposition method between the conductor glass and the nanocrystalline TiO_2 film also works well.[21,22] It is believed that these improvements of the performance in the solar cell are due to the suppression of the dark current at the semiconductor electrolyte junction and a decrease in the ohmic loss between the conducting layer and the nanocrystalline TiO_2 films. In our case, it has been expected that the contact between the nanorod layer and the glass substrate would be poor due to the larger diameter and length of the nanorods, which may leave more free-contact space on the surface of glass and increase the ohmic loss. Accordingly, one double-layer structural cell has been designed to optimize the electricity contiguity between the nanorod film and the conductor layer. First, a compact TiO_2 layer prepared by the sol−gel method was coated and calcined to form a layer with a thickness of below 1 μm, and then a nanorod film was directly coated on the surface of the layers followed by calcination again to form a nanorod film. Figure 8 shows the *I*−*V* curve of the optimized nanorod cell with a thickness of 13.7 μm. When the performance of the nanorod cell without the compact optimized layer is compared, it is clear that the photocurrent density is as high as 13.1 mA/cm^2 even with the thinner film, and the V_{oc} also shows a higher value of 0.767 V. And the fill factor increases to 0.728, which also indicates that ohmic loss is restrained with the compact TiO_2 layer. The efficiency of the double-layer cell is as high as 7.29%. It needs to be mentioned that the amount of dye adsorbed in the nanorod film is not drastically increased as compared with the P-25 cell (Figure 5), which is attributed to be mainly due to the larger size of the nanorods. However, the TiO_2 nanorod DSSC can be expected to adsorb more dyes when the diameter of the rods decreased to a small size. In addition to the rapid transportation of electrons, a high conversion efficiency of light-to-electricity will be achieved with nanorod TiO_2 film.

Conclusion

Single-crystalline anatase TiO_2 nanorods were successfully synthesized by a surfactant-assisted hydrothermal method. A high light-to-electricity conversion yield of 7.29% was achieved by applying the titania as a thin film in dye-sensitized solar cells.

Acknowledgment. This work was supported by the Strategic University/Industry Alliance of the International Innovation Center, Kyoto University. The conductive ITO was kindly donated by Geomatec Co. Ltd.

References and Notes

(1) O'Regan, B.; Grätzel, M. *Nature* **1991**, *353*, 737.
(2) Adachi, M.; Murata, Y.; Takao, J.; Jiu, J.; Sakamoto, M.; Wang, F. *J. Am. Chem. Soc.* **2004**, *126*, 14943.
(3) Papageogiou, N.; Barb, C.; Grätzel, M. *J. Phys. Chem. B* **1998**, *102*, 4156.
(4) Gómez, M.; Lu, J.; Olsson, E.; Hagfeldt, A.; Granqvist, C. G. *Sol. Energy Mater. Sol. Cells* **2000**, *64*, 385.
(5) Horiuchi, T.; Miura, H.; Uchida, S. *Chem. Commun.* **2003**, 3036.
(6) Barzykin, A. V.; Tachiya, M. *J. Phys. Chem. B* **2004**, *108*, 8385.
(7) Kay, A.; Grätzel, M. *Chem. Mater.* **2002**, *14*, 2930.
(8) Dresselhausa, M. S.; Linb, Y. M.; Rabinc, O.; Jorioa, A.; Souza Filhoa, A. G.; Pimentad, M. A.; Saitof, R.; Samsonidzeb, Ge. G.; Dresselhausg, G. *Mater.Sci. Eng., C* **2003**, *23*, 129.
(9) Jiu, J.; Wang, F.; Sakamoto, M.; Takao, J.; Adachi, M. *J. Electrochem. Soc.* **2004**, *151*, A1653.
(10) Sugimoto, T.; Zhou, X. P.; Muramatsu, A. *J. Colloid Interface Sci.* **2003**, *259*, 53.
(11) Lei, Y.; Meng, L. D.; Meng, G. W.; Li, G. H.; Zhang, X. Y.; Liang, C. H.; Chen, W.; Wang, S. X. *Appl. Phys. Lett.* **2001**, *78*, 1125.
(12) Kasuga, T.; Hiramatsu, M.; Hoson, A.; Sekino, T.; Niihara, K. *Langmuir* **1998**, *14*, 3160.
(13) Puntes, V. F.; Krishnan, K. M.; Alivisatos, A. P. *Science* **2001**, *291*, 2115.
(14) Jun, Y.; Casula, M. F.; Sim, J.; Kin, S. Y.; Cheon, J.; Alivisatos, A. P. *J. Am. Chem. Soc.* **2003**, *125*, 15981.

(15) Penn, R. L.; Banfield, J. F. *Geochim. Cosmichim. Acta* **1999**, *63*, 1549.
(16) Donnay, J. D.; Harker, D. *Am. Mineral.* **1937**, *22*, 446.
(17) Barnard, A. S.; Zapol, P. *J. Phys. Chem. B* **2004**, *108*, 18435.
(18) Shklover, V.; Ovchinnkov, Yu. E.; Braginsky, L. S.; Zakeeruddin, S. M.; Grätzel, M. *Chem. Mater.* **1998**, *10*, 2533.
(19) Grätzel, M. *Pure Appl. Chem.* **2001**, *73*, 459.
(20) Barbe, C. J.; Arendse, F.; Comte, P.; Jirousek, M.; Lenzmann, F.; Ahklover, V.; Grätzel, M. *J. Am. Chem. Soc.* **1997**, *80*, 3157.
(21) Bach, U.; Lupo, D.; Comte, P.; et al. *Nature* **1998**, *395*, 583.
(22) Gómez, M. M.; Lu, J.; Olsson, E.; Hagfeldt, A.; Granqvist, C. G. *Sol. Energy Mater. Sol. Cells* **2000**, *64*, 385.